Realization of a 10 MHz integrated bipolar DECT band-pass filter

Peter M. Stroet, Paul T. M. van Zeijl+, Roelof F. Wassenaar**

*MESA Research Institute University of Twente
P.O. Box 217, 7500 AE Enschede
The Netherlands
phone: x-31-53-4892732
fax: x-31-53-4892799

+Ericsson Mobile Networks B.V.
Institutenweg 25
P.O. Box 645, Enschede
The Netherlands

Abstract- **In this paper an eight-order continuous-time Butterworth band-pass filter with quality factor of 10 is presented, intended to be used for selectivity in modern DECT handset receivers. A distortion analysis is performed and a model to describe the frequency dependent Spurious-Free Dynamic-Range (SFDR) in absolute value is presented. Measurements show a SFDR of 48 dB with a 3 mW power consumption.**

I. Introduction

Until now, Surface-Acoustic-Wave (SAW) filters are frequently used in DECT handset receivers for selectivity. However, they have some disadvantages: the relatively large package, the fixed input-output impedance, the insertion loss and the high cost. The aim of the filter to be presented is to beat these disadvantages by integrating selectivity along with other radio circuits. These radio circuits are already realized in a high-frequency bipolar process, and therefore, the integrated filter must be bipolar too.

Digital filters require A/D-converters with a considerable power consumption and moreover they need analog anti-aliasing filters. This paper discusses a continuous-time g_m/C band-pass filter, that does not require this overhead. In section II, the filter design is given. Special attention is paid to the scaling, the linearization and the low-noise performance.

Compared to SAW-filters, active integrated filters have a poor ratio between dynamic range and consumed supply power. For an acceptable power consumption, dynamic range is a problem. The upper bound of the dynamic range is determined by inter-modulation distortion, and the lower bound by noise. To express filter quality regarding to these bounds, the SFDR definition [1] is used. In section III the SFDR measurements and modeling are given. In contrast to former work, the *absolute* value of the SFDR can be calculated with the model presented in this paper. In addition, a *more accurate* SFDR modeling of capacitive coupled band-pass filters with a *low Q* ($Q < 20$) is given. An eight-order Butterworth band-pass filter is chosen, as a trade-off between selectivity and group-delay ripple. The center frequency f_0 is 10 MHz and the required -3 dB bandwidth of 1 MHz results in a quality factor $Q = 10$.

II. Filter design

The eight-order filter structure (Fig. 1) consists of four capacitive coupled resonators, with termination resistors at the input (R_S) and output (R_L). Each resonator is implemented by two anti-parallel transconductors connected with capacitors (Fig. 2). All circuits are balanced, in order to improve common-mode and power-supply rejection. All resonator capacitors (this is C_1 for the first resonator in Fig. 2) are split into a common part (C_a), needed to avoid

common-mode instability, and a differential part (C_b). In comparison with the case of using common capacitors C_a only, a reduction of capacitor chip area is achieved. Also a faster startup behavior is realized because of the reduced common part, forming a time-constant with the relatively high common-mode output resistance of the transconductors. An oscillator, matched with the resonator, is designed to extract frequency and amplitude information in order to tune the filter according to the Master-Slave principle [2]. Each transconductor is implemented as shown in Fig. 3. The common-mode feedback circuit is not drawn. Emitter-degeneration is used for transconductor linearization. The frequency tuning is realized by switching on or off an array of parallel emitter-degenerated differential pairs [3]. The resonator quality factor is determined by R_q, C_q (Fig. 3) and the emitter resistance of the input transistors T1 and T2. Therefore, Q-tuning can easily be realized by adjusting the biasing current (I_q) of these input transistors. R_q is chosen 150 kΩ to set the phase of the transconductor-capacitor combination to -90° at f_0 for I_q = 17 µA. Varying I_q results in a phase tuning range from -91.0º up to -89.0°. All transconductors are equal and identically biased to facilitate good matching and to provide an equal input-voltage range of every stage. To be able to compensate for component tolerances without altering the transfer function, the resistors R_S and R_L (Fig. 1) should track along with $1/g_m$ (where g_m equals the transconductor transconductance). This problem is solved by implementing R_S with M2, R_{qa} and R_{qb} (see Fig. 2). As a result, the total noise increases with 3.5 dB.
The filter is implemented in a 15 GHz f_T bipolar process from Ericsson Components. The supply voltage is 3 to 5.5 V, and 6.8 mA total current is drawn. By enabling the filter during the desired time-slot only [4], a 724 µA total average current is measured. Figure 4 presents the layout with a chip area of 2.6 mm². The simulated and measured filter transfer is shown in Fig. 5. Vn1...Vn4 denote the voltage on the nodes n1...n4 in Fig. 1.

III. Spurious-Free Dynamic-Range (SFDR)

For DECT applications, very important specifications are the inter-modulation distortion and the noise [4] because in most cases, they will determine the dynamic range. Therefore, the SFDR is a good figure of merit for a filter because both the inter-modulation distortion performance and the noise performance are included. We call the power of two input signals at frequencies $f_1 = f_0 + \Delta f$ and $f_2 = f_0 + 2 \cdot \Delta f$ as P_{in}, for each signal (Fig. 6). These two signals generate an output inter-modulation component (P_{imc}) in the center of the pass-band. The Spurious-Free Dynamic-Range can be defined as:

$$SFDR = \left. \frac{P_{in} \cdot G_{fd}}{P_{noise,out}} \right|_{P_{noise,out} = P_{imc}} \tag{1}$$

with G_{fd} the pass-band power gain and $P_{noise,out}$ the output noise. The condition for this definition is that for a certain (high) P_{in}, the resulting P_{imc} equals $P_{noise,out}$. This SFDR is measured for various Δf, see Fig. 7. It can be deduced, although the filter slope is 24 dB/octave that the SFDR(Δf) has a slope of approximately 6 dB/octave. This behavior is caused by non-linearities in the first resonator (Fig. 2). A similar behavior has been reported before [1]. In contrast to former work, a modified model is presented in this paper giving the frequency dependent SFDR in *absolute* terms that can be calculated from the basic components, assuming the use of equal transconductor-capacitor sections. The filter noise is calculated to be:

$$P_N \approx 10 \cdot \log(8kT \cdot 1/g_m \cdot NEF_t \cdot f_0 \cdot Q \cdot n) \tag{2}$$

with k Boltzmann's constant, T absolute temperature, NEF_t transconductor Noise Excess Factor, f_0 filter center frequency, Q quality factor of the total filter and n the low-pass equivalent filter order (≡ half times the band-pass filter order). Assuming $Q \geq 2$, $n \geq 2$, B the -3 dB bandwidth, the SFDR is given by:

$$SFDR(f_1) \approx \frac{2}{3}\cdot(IP3_T - P_N - 6) + 20\cdot\log(\frac{f_0 - f_1}{f_0 - f_{ZL}}\cdot\frac{2\cdot f_{ZL}}{f_{ZL} + f_1}) - 3 \qquad [dB] \quad f_1 < f_0 - \tfrac{1}{2}B \quad (3)$$

$$SFDR(f_1) \approx \frac{2}{3}\cdot(IP3_T - P_N - 6) + 20\cdot\log(\frac{f_1 - f_0}{f_{ZH} - f_0}\cdot\frac{f_{ZH}}{f_1}) \qquad [dB] \quad f_1 > f_0 + \tfrac{1}{2}B \quad (4)$$

The transconductor intercept point $IP3_T$ is used to determine the distortion. The frequency f_Z of the filter is defined as the frequency where the transfer function $2\cdot Vn1/Vin$ is crossing the 0 dB axis (Fig. 5), resulting in f_{ZH} for the upper side and f_{ZL} for the lower side. Most band-pass filters with $Q \geq 2$ will give higher gain at node 1 at the edges of the band-pass.
For low Q filters ($Q < 20$), the AC transfer will be significantly asymmetric due to the use of coupling capacitors C12, C23 and C34 (Fig. 1). This results in a less sharp cut-off behavior for the high frequency side of the pass-band and a sharper cut-off for the low frequency side. This asymmetry is also seen for the inter-modulation distortion, which is mainly determined by the first node voltage (*Vn1*). Therefore, an extra frequency dependent term (f_1) is used in (3) and (4) compared to former work [1]. In formula (3) and (4) a 6 dB degradation of the $IP3_T$ is found because *Vn1* and *Vn1b* (Fig. 2) are equal in magnitude and thus an equal inter-modulation contribution of both M3 and M4 is expected. Because both inter-modulation contributions are correlated, the worst case degradation of 6 dB is used. For high values of $|\Delta f|$, an asymptote in the SFDR is reached, caused by clipping in the first transconductor M1 (Fig. 2). For a correct design, approximately $20\cdot\log(Q/2)$ improvement above SFDR(f_{ZH}) can be reached. In Fig. 7 the measurement results, the old model [1] and the modified model are given for SFDR(f_1). A better fit is achieved with the modified model. In formula (3) an extra -3 dB is added compared to (4), probably caused by the effect that for $f_1 > f_0 + \frac{1}{2}B$ attenuation is performed directly by C_a and C_b (Fig. 2), while for $f_1 < f_0 - \frac{1}{2}B$ a signal path through M3 and M4 is required to create attenuation. From the simulation and measurement results can be concluded that the filter performance is very close to the DECT requirements [4]. A critical specification for a DECT selectivity filter is the in-pass-band inter-modulation distortion caused by the second and the fourth neighbor channels. A SFDR of 48 dB is measured which is close to this DECT requirement [4].
For the sake of completeness, the Blocking Dynamic-Range (BDR) as defined in [1] is measured and given in Fig. 7. In the near future, measurements with a DECT receiver will give detailed information about the filter over-all performance.

IV. Conclusion

Realizing selectivity in DECT receivers by using an integrated continuous-time gm/C-filter (with an acceptable power consumption for handsets) is within reach. The Spurious-Free Dynamic-Range (SFDR) specifies filter quality. The more the out-of-pass-band frequencies are away from the filter center-frequency, the higher the SFDR becomes. However, the improvement is less than what would be expected from a fourth-order roll-off. A model is presented giving the absolute value of the SFDR. For low-Q filters a better fit of SFDR(f) is found compared to former work. For the second and fourth neighbor channels, a SFDR of 48 dB is measured with a 3 mW power consumption.

V. Acknowledgment

Authors like to acknowledge Ericsson Components, Kista Sweden, for processing the ASIC, A. Sluik for CAD support, J. Geerlings for the photograph and J. C. Kuenen for his assistance.

VI. References

[1] W. B. Kuhn, F. W. Stephenson, A. Elshabini-Riad, "A 200 MHz CMOS Q-Enhanced LC Band-pass Filter," IEEE Journal of solid-state circuits, vol. 31, no. 8, pp. 1112-1121, august 1996.
[2] J. R. Canning and G. A. Wilson, "Frequency discriminator circuit arrangement," U.K. pat. 1 421 093, January 1976.
[3] R. Castello, "Low-Voltage Continuous-Time Filters" (Fig. 10), Proceedings of the Workshop on Advances in Analog Circuit Design, Lausanne, Switzerland, April 2-4, 1996.
[4] TBR6, Digital European Cordless Telecommunications, General Terminal Attachments Requirements, ETSI, June 1996.

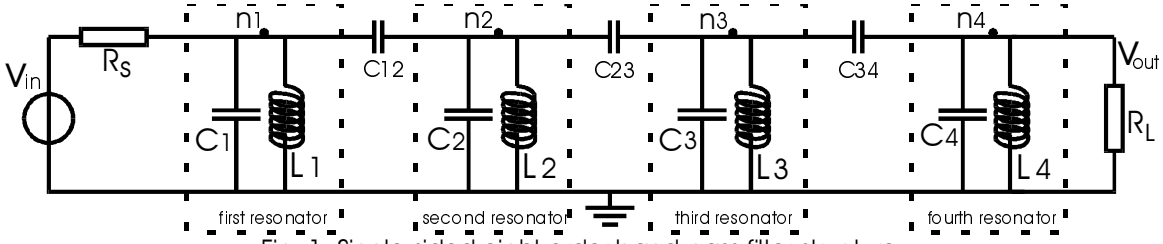

Fig. 1: Single-sided eight-order band-pass filter structure

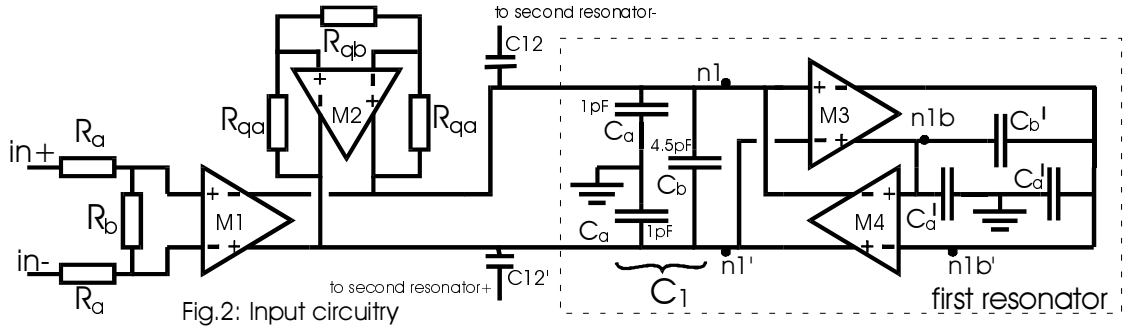

Fig.2: Input circuitry

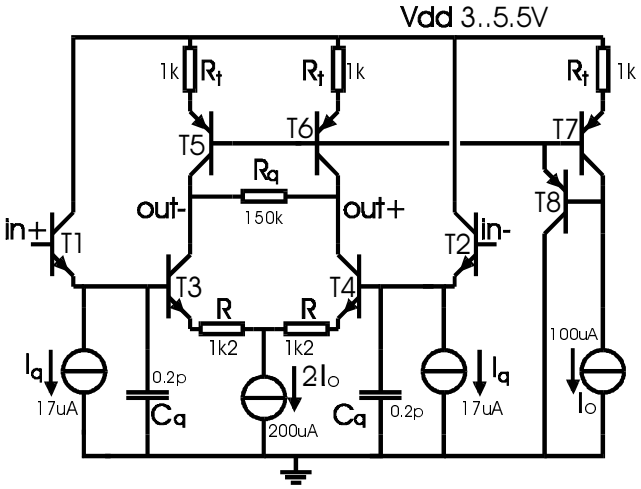

Fig.3: transconductor design

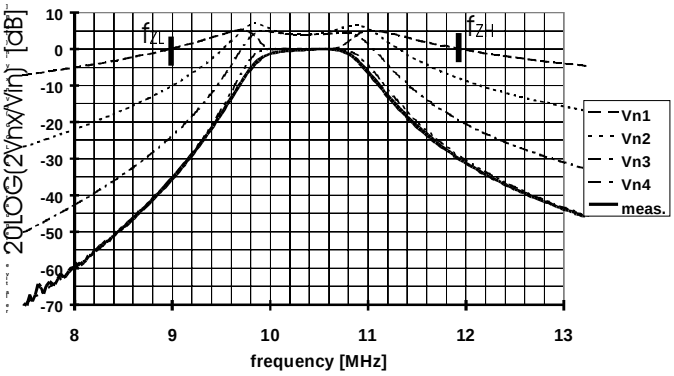

Fig. 5: Measurement and simulation of the transfer functions

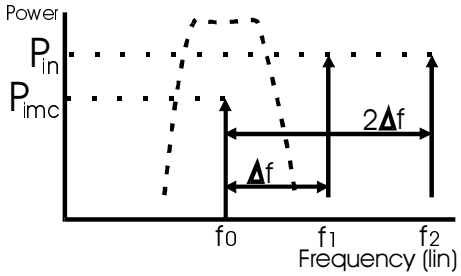

Fig.6:
the input power (Pin) spectrum, the IM3 output power (Pimc) spectrum with indicated the band-pass curve

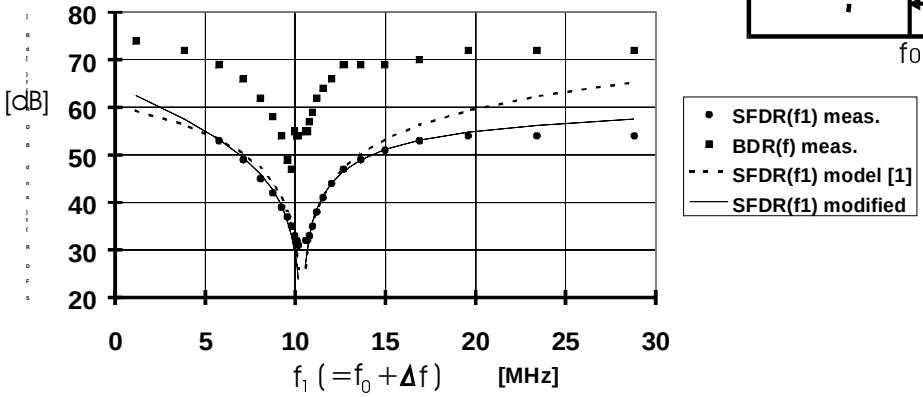

Fig. 7: Measured and modeled Spurious-Free Dynamic-Range (SFDR) and measured Blocking Dynamic Range (BDR)

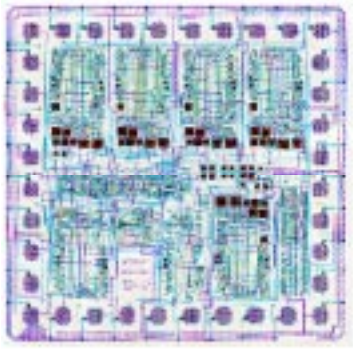

Fig. 4: chip photograph